1	Mapping the Role of Efflux Pumps in the Evolution of Antibiotic Resistance Reveals Near-
2	MIC Treatments Facilitate Resistance Acquisition
3	
4	Ariel M. Langevin ^{a,b} , Imane El Meouche ^{a,b,*} , Mary J. Dunlop ^{a,b,#}
5	
6	^a Department of Biomedical Engineering, Boston, Massachusetts, USA
7	^b Biological Design Center, Boston, Massachusetts, USA
8	
9	Running Head: Efflux pumps and resistance evolution
10	
11	[#] Address correspondence to Mary J. Dunlop, mjdunlop@bu.edu
12	* Present address: Imane El Meouche, Université de Paris, IAME, UMR1137, INSERM, Paris,
13	France
14	
15	Word count of Abstract: 249

16 Word count of Manuscript: 4,141

17 ABSTRACT

18 Antibiotic resistance has become a major public health concern as bacteria evolve to evade 19 drugs, leading to recurring infections and a decrease in antibiotic efficacy. Systematic efforts 20 have revealed mechanisms involved in resistance; yet, in many cases, how these specific 21 mechanisms accelerate or slow the evolution of resistance remains unclear. Here, we conducted a 22 systematic study of the impact of the AcrAB-TolC efflux pump and its expression on the 23 evolution of antibiotic resistance. We mapped how population growth rate and resistance change 24 over time as a function of both the antibiotic concentration and the parent strain's genetic 25 background. We compared strains lacking functional AcrAB-TolC efflux pumps, the wild type 26 strain, and those overexpressing the pumps. In all cases, resistance emerged when cultures were 27 treated with chloramphenicol concentrations near the MIC of the parent strain. Strains grown in 28 concentrations just above the MIC were the most prone to evolving high levels of drug 29 resistance, in some cases reaching values that far exceed the concentrations they were treated 30 with. The genetic background of the parent strain also influenced resistance acquisition. The 31 strain overexpressing pumps evolved resistance more slowly and at lower levels than the wild 32 type strain or the strain lacking functional pumps. In contrast, the wild type strain rapidly 33 achieved resistance through mutations in pump genes and their associated regulators. Overall, 34 our results suggest that treatment conditions just above the MIC pose the largest risk for the 35 evolution of resistance, and precise control of pump expression levels accelerates this process.

36

37 **IMPORTANCE**

38 Combatting the rise of antibiotic resistance is a significant challenge. Efflux pumps are an 39 important contributor to drug resistance, and they exist across many cell types and can export

40 numerous classes of antibiotics. Cells with efflux pumps can regulate pump expression to 41 maintain low intracellular drug concentrations. Here, we explored a three-dimensional 42 evolutionary landscape, in which we mapped how resistance emerged depending on the 43 antibiotic concentration, the presence of efflux pumps and their regulators, and time. We found 44 that treatments just above the antibiotic concentration that inhibits growth of the parent strain 45 were most likely to promote resistance, but that efflux pump levels influence the severity of these 46 outcomes. These results indicate that there are specific treatment regimens and strain 47 backgrounds that are especially problematic for the evolution of resistance.

48

49 INTRODUCTION

50 Despite the new wave of antibiotic discovery (1–5), bacteria continue to acquire resistance 51 shortly after the introduction of new drugs for medicinal and industrial applications (6, 7). This is 52 due in large part to the overuse of antibiotics, which results in pressures that drive resistance (8). 53 With limited novel antibiotics and numerous futile antibiotics, doctors and scientists alike are 54 presented with the challenge of how to best treat infections while keeping the evolution of 55 resistance in check.

56

Adaptive evolution studies have begun exploring how certain antibiotic pressures influence the evolution of resistance. For instance, studies using a 'morbidostat'—a continuous culture device that dynamically adjusts antibiotic concentrations to inhibitory levels—have found numerous targets that can be readily mutated to promote resistance (9–11), as well as identifying how drug switching can limit the evolution of resistance (12). While these studies have provided pivotal insights for this field, the morbidostat design causes antibiotic concentrations to rise to levels that exceed clinically relevant concentrations due to toxicity for patients (13). In recognition of the drug concertation-dependent nature of evolution, researchers have begun to explore bacterial evolution under treatment conditions with lower antibiotic concentrations as well. Wistrand-Yuen *et al.* found that bacteria grown in sub-inhibitory drug concentractions were still able to achieve high levels of resistance (14–16). Notably, the study identified that the same antibiotic produced unique evolutionary pathways when cells were treated with sub-inhibitory concentrations as opposed to inhibitory concentrations (14).

70

71 One limitation of current studies within the field is that they can be difficult to compare due to 72 variations in experimental parameters, such as species, antibiotics, or other experimental 73 conditions (17). Given the unique evolutionary pathways at different antibiotic concentrations, 74 systematic mapping of these evolutionary landscapes could provide an improved understanding 75 of which conditions pose the highest risk by allowing direct comparisons between different 76 antibiotic concentrations. For instance, evolution experiments that were conducted using a range 77 of concentrations for beta-lactams (18) and erythromycin (19) have highlighted the 78 concentration-dependent adaptability of Escherichia coli.

79

There are many mechanisms by which antibiotic resistance can be achieved, including enzymatic inactivation, alteration of antibiotic binding sites, and increased efflux or reduced influx of antibiotics (20, 21). Efflux pumps are omnipresent in prokaryotic and eukaryotic cells alike, and are an important contributor to multi-drug resistance (22). AcrAB-TolC in *E. coli* is a canonical example of a multi-drug efflux pump, providing broad-spectrum resistance and raising the MIC of at least nine different classes of antibiotics (23). The pump is composed of three types of

proteins: the outer membrane channel protein, TolC; the periplasmic linker protein, AcrA; and the inner membrane protein responsible for substrate recognition and export, AcrB (22). Using the proton motive force, AcrB actively exports antibiotics from the cell (22, 24). The presence of AcrAB-TolC efflux pumps can increase a strain's MIC from ~2-fold to ~10-fold, depending on the antibiotic (25–27). Furthermore, genes associated with these multi-drug resistant efflux pumps, including their local and global regulators, are common targets for mutation as strains evolve high levels of drug resistance (15, 28–31).

93

94 Recent studies have indicated that in addition to providing modest increases in the MIC due to 95 drug export, pumps can also impact mutation rate and evolvability of strains, which may 96 ultimately be more important for the acquisition of high levels of drug resistance. For example, 97 heterogeneity in efflux pump expression can predispose subsets of bacterial populations to 98 mutation even prior to antibiotic treatment (32). In addition, deleting genes associated with 99 efflux pumps can also reduce evolvability under antibiotic exposure (33). These studies provoke 100 the question of how efflux pumps, and their expression levels, can serve to promote or attenuate 101 the evolution of drug resistance. To address this, we mapped the progression of resistance over 102 time for strains with and without efflux pumps and their native regulator.

103

Our overall goal in this study was to identify how antibiotic resistance emerges based on the antibiotic concentration, the parent strain's genetic background, and the time since treatment. To achieve this, we used a turbidostat as an evolutionary platform (34) and treated cultures with a range of chloramphenicol concentrations. Chloramphenicol is often used as a last resort antibiotic in multi-drug resistant infections, as most clinical isolates are still susceptible to this

109 drug (35, 36). We measured the effect of various genetic backgrounds with different pump 110 expression levels. We conducted these tests in a strain lacking functional AcrAB-TolC efflux 111 pumps ($\Delta acrB$); in the wild type strain with the native regulatory network controlling AcrAB-112 TolC expression (WT); and in a strain with upregulated expression of the pumps (37), which 113 lacks the local regulator AcrR (AcrAB+). We allowed the cultures to grow and evolve for 72 h in 114 continuous culture while continuously recording growth rates. We periodically sampled the 115 cultures and assessed the population's resistance. We then charted the evolutionary landscapes 116 under different antibiotic concentrations, genetic backgrounds, and through time and identified 117 which circumstances gave rise to resistance.

118

119 **RESULTS**

In order to systematically evaluate the evolutionary landscape of efflux pump-mediated antibiotic resistance, we used the eVOLVER, a modular turbidostat capable of growing independent cultures in parallel (34). This platform allowed us to track a culture's fitness by measuring growth rate continuously over multi-day experiments. In addition to this, we collected samples at selected intervals and, with these samples, performed antibiotic disc diffusion assays to assess the population's resistance and spot assays to quantify the presences of high-resistance isolates within the population (Figure 1).

127

We mapped growth rates over time for cultures subjected to a range of chloramphenicol treatment concentrations (Figure 2A & Figure S1). Treatment with high concentrations of chloramphenicol repressed bacterial growth for multiple days. We observed this growth inhibition for chloramphenicol concentrations >5x MIC⁰, where we define MIC⁰ as the MIC of

132 the parent strain. Cultures grown in lower chloramphenicol concentrations were able to recover 133 growth. For example, when we treated the bacterial populations with concentrations that were at or above MIC^0 but below 5x MIC^0 , we observed a significant decrease in the growth rate 134 135 between 0 and 12 h. However, after 12 to 24 h, growth in these populations was partially restored. Below MIC⁰, cultures were able to grow, though usually at a deficit compared to 136 137 conditions without chloramphenicol. Growth recovery results for the three strains ($\Delta acrB$, WT, and AcrAB+) were qualitatively similar when normalized by the MIC⁰ value. As such, complete 138 139 growth inhibition occurred at a lower chloramphenicol concentration in the $\Delta acrB$ strain than in 140 WT or AcrAB+, although overall recovery patterns were similar.

141

142 The growth rate results suggested the evolution of drug resistance within the population. To 143 quantify this, we used an antibiotic disc assay to map the corresponding resistance levels (Figure 144 2B & Figure S2). We found distinct increases in resistance levels that corresponded to 145 populations which recovered growth. While there were qualitative similarities for the three 146 strains, the timing and level of resistance achieved was dependent on the strain background. The 147 WT strain was able to rapidly achieve high levels of resistance for a broad range of 148 chloramphenicol treatment concentrations. Resistance generally emerged within 12-24 h for concentrations that ranged from below MIC⁰ up to 5x MIC⁰. In contrast, the $\Delta acrB$ cells 149 150 achieved resistance more slowly, but were ultimately able to reach levels of resistance 151 comparable to the WT strain. Resistance acquisition for $\Delta acrB$ occurred within a comparatively small range of chloramphenicol concentrations, centered just above MIC⁰. The AcrAB+ strain, 152 153 where efflux pumps are overexpressed, was able to evolve resistance, though this occurred more 154 slowly and under a narrower range of treatment concentrations than in the WT strain.

155

156 To compare the ultimate resistance levels for the three strains, we calculated the final MIC of the populations at 72 h (MIC^f). We found that treatments concentrations $\sim 2x$ MIC⁰ produced the 157 158 most resistant populations (Figure 2C). The selective pressures of sub-inhibitory antibiotic 159 concentrations have often been considered high-risk for the evolution of resistance (14, 38). Yet, our results indicated that concentrations near or just above MIC⁰ lead to the highest resistance 160 161 levels in these conditions. While the range of raw chloramphenicol values that support the evolution of resistance varied between the strains, when we normalized by MIC⁰, AcrAB+ had 162 163 the narrowest region of chloramphenicol concentrations that resulted in resistance. These results 164 suggest that AcrAB+ has a reduced capacity to evolve resistance relative to the other strains.

165

166 We next asked how resistance and growth changed through time. We found that in the absence 167 of antibiotics, the trajectories trended largely towards faster growth, with minimal changes to resistance levels (Figure 3). With sub-MIC⁰ chloramphenicol treatment, we observed that the 168 populations first experienced a slight growth decrease, followed by increased resistance, and then 169 170 restored growth within 48 h. While these populations did gain resistance, they did not tend to reach very high MIC^f values. In contrast, at 1x and 2x MIC⁰ chloramphenicol treatment, there 171 172 was a more dramatic reduction in growth within the first 12 h. Though growth was impacted, the 173 populations tended to walk towards high resistance during this period. As depicted in the 174 schematics, the zig-zag patterns trending towards high resistance may be indicative of the 175 cultures acquiring resistant mutations and compensating for the associated fitness costs of these mutations. Finally, bacteria treated with 10x MIC⁰ first became more susceptible and then 176 177 stopped growing entirely within 12 h; growth was never restored for these populations. We found that strains from all three genetic backgrounds followed similar evolutionary trajectories while balancing the trade-off between growth and resistance. These findings highlight the importance of using antibiotic concentrations that are sufficiently inhibitory.

181

182 While these results tell us about the growth rate and resistance of the overall population, it is 183 difficult to determine if sub-populations of cells within the culture have acquired high levels of 184 resistance from disc assays alone. First, because the disc assays do not quantify resistance 185 associated with individual cells in the culture, they cannot reveal the presence of subpopulations 186 of resistant and susceptible cells. Second, beyond a certain resistance level, cells will grow up to 187 the boundary of the disc; thus, it is not possible to quantify resistance increases beyond this. 188 Determining which conditions can give rise to high levels of resistance is important for revealing 189 particularly dangerous treatment regimes. In addition, sub-populations with increased resistance 190 to one antibiotic can promote cross-resistance to other drugs (38).

191

192 To quantify the fraction of resistant cells that emerged during our evolution experiment, we 193 conducted a spot assay, in which we measured the fraction of the population capable of surviving 194 on specific chloramphenicol concentrations. For all three strains, we observed sub-populations 195 that were capable of growing on 10 μ g/mL chloramphenicol (Figure 4A & Figure S3). 196 Interestingly, these cells primarily emerged from treatment conditions with lower levels of 197 chloramphenicol, and not from conditions where cells were subjected to 10 µg/mL 198 chloramphenicol. For example, over 5% of the population from each of the three WT replicates 199 that were treated at 2 μ g/mL chloramphenicol could survive on 10 μ g/mL at the end of the 200 experiment. We did find cases where WT cells treated with 10 µg/mL evolved resistance to 10 μ g/mL, however this was less common than in treatments near MIC⁰. Thus, cultures were able to evolve resistance to higher levels of chloramphenicol than they were subjected to, a feature that was most pronounced when treatments were just above or at MIC⁰. These results closely match trends in the population's overall resistance (Figure 2B). We also found isolates capable of growing on 20 µg/mL chloramphenicol, with a reduced frequency relative to 10 µg/mL (Figure 4B & Figure S3-S4).

207

208 Interestingly, the $\Delta acrB$ strain consistently produced sub-populations that were able to grow at 20 µg/mL (or 40x MIC⁰) chloramphenicol by 72 h. This sub-population appeared for 209 210 chloramphenicol concentrations around 2 µg/mL. WT results followed a similar trend, with 211 resistance to both 10 and 20 µg/mL chloramphenicol evolving by 72 h. In contrast, the AcrAB+ 212 strain was capable of evolving resistance to 10 µg/mL when treated with chloramphenicol concentrations slightly above MIC⁰; yet, AcrAB+ never produced a sub-population that was able 213 214 to grow on 20 µg/mL as the other strains did. These results were consistent with our findings that 215 AcrAB+ is less prone to evolve high levels of resistance than the $\Delta acrB$ or the WT strains are.

216

A key question remained: which mutations were responsible for the increases in resistance we observed? To address this, we used whole genome sequencing to analyze three biological replicates from the 72 h timepoint for the WT strain (Figure S5). All of the sequenced isolates had a point mutation in the DNA binding region of *marR*, which can upregulate AcrAB-TolC efflux pumps and expression of other stress response genes (39). Additionally, two isolates had an IS1 or IS5 insertional sequence interrupting *acrR*, which would upregulate *acrAB* (40). The other isolate had a single point mutation in a periplasmic encoding region of *acrB*, in close proximity to a site found to aid in chloramphenicol resistance (41, 42). These sequencing results indicate that strains containing AcrAB-TolC efflux pumps use mutations related to the pumps and their regulation to optimize survival and increase resistance in the presence of antibiotics.

227

228 **DISCUSSION**

In this work, we identified that treating strains with antibiotic concentrations close to MIC^{0} is 229 230 problematic for the evolution of resistance; however, the evolvability and ultimate resistance 231 level achieved depend heavily on the genetic background. For $\Delta acrB$, WT, and AcrAB+ strains, 232 we observed some common features between the evolutionary landscapes, where reductions in 233 growth rate were followed by increases in resistance. Yet, despite qualitative similarities, the 234 degree to which these strains became resistant depended on the presence of AcrAB-TolC efflux 235 pumps. WT bacterial populations with access to precise control of resistance machinery (i.e. 236 efflux pumps and control of stress response regulators), evolved mutations that conferred high 237 levels of resistance within 48 h after antibiotic exposure. The three biological replicates 238 developed similar mutations in marR, acrR, and acrB to upregulate AcrAB-TolC efflux pumps in the WT strain, resulting in a population capable of surviving 10x MIC⁰ chloramphenicol 239 240 treatment. These results are consistent with findings from drug resistance studies that have 241 identified point mutations and insertional sequences in regulators that serve to upregulate efflux 242 pumps (11, 24, 43-45). Notably, AcrAB+, which overexpresses efflux pumps, was less 243 evolvable and never achieved as high levels of resistance as the WT strain, suggesting that both 244 having pumps and the ability to precisely control their expression together are important in the 245 evolution of resistance. This reduced evolvability of AcrAB+ may be a result of the fitness 246 burden of constitutive pump overexpression (25, 46). In contrast, we found that under certain 247 conditions the $\Delta acrB$ strain evolved to survive on 40x MIC⁰. This phenomenon agrees with 248 results by Cudkowicz & Schuldiner, who found that evolving $\Delta acrB$ produced a more resistant 249 population than evolving WT. They showed that the $\Delta acrB$ strain gained high resistance by 250 optimizing redundant efflux pumps in *E. coli*, such as AcrEF and MdtEF (11). Taken together, 251 these findings suggest that carefully modulating the exact levels of pump expression may be 252 critical for evolving resistance.

253

254 Our results identify antibiotic treatment regimes that are especially prone to mutation. While 255 doctors measure resistance of bacterial infections, they sometimes prescribe antibiotic treatment 256 prior to obtaining the results of this assay (47) or use a treatment concentration too low to 257 effectively penetrate an infection site (48). This blind treatment could lead to increased levels of 258 resistance (49, 50). Yet, potentially more dangerous are the differences between the simulated 259 plasma-concentration and measured plasma-concentrations of patients. In a study at the Kenya 260 Medical Research Institute, patients were administered a concentration of chloramphenicol well 261 above the MIC for the Streptococcus pneumoniae being treated (51). Researchers simulated the 262 administered dosing regime and later measured the plasma-concentration; their findings 263 demonstrated that the true concentration of chloramphenicol in the patients was often 2-5x MIC, 264 as opposed to the 5-10x MIC anticipated. These findings are relevant in that we found that in 265 vitro chloramphenicol treatments under 10x MIC, especially 1-2x MIC treatments, most readily 266 promote the emergence of highly resistant bacterial populations. Reding et al. similarly observed 267 this hotspot for adaptability of *E. coli* in the presence of another antibiotic, erythromycin, just 268 below its MIC (19). Although it is essential for healthcare workers to be mindful of toxicity and

accessibility, our results highlight the presence of regimes that are especially problematic andwhich should be avoided to limit evolution of antibiotic resistance.

271

By charting evolutionary landscapes across different antibiotic concentrations, different parent strains, and time, we have gained insight into treatments that impact the emergence of antibiotic resistance and the role of efflux pumps in this process.

275

276 **METHODS**

277 Strains and Plasmids

278 We used E. coli strains BW25113 (WT), BW25113 $\triangle acrB$ ($\triangle acrB$), and BW25113 $\triangle acrR$ 279 (AcrAB+). The wild type strain BW25113 is the parent strain for the Keio collection (52). 280 BW25113 $\triangle acrB$ was derived from Keio collection strain JW0451 (BW25113 $\triangle acrB::kan^R$) 281 (25). For BW25113 $\Delta acrR$, we designed primers with homology regions on acrR and amplified 282 the kanamycin resistance marker and FRT sites of pKD13 (52). Primers are listed in Table S1. 283 The linear DNA was then treated using a DpnI digest and PCR purification. We electroporated 284 the purified linear DNA into competent BW25113 cells containing the plasmid pSIM6 (53). We 285 removed kanamycin resistance markers following the pCP20 protocol from Reference (54).

286

Determination of MIC

For all experiments, overnight cultures were inoculated from a single colony in 10 mL LB and grown in a 50 mL Erlenmeyer flask at 37°C with 200 rpm orbital shaking. After overnight growth, the optical density at 600 nm (OD_{600}) was measured, and the initial volume was diluted back to $OD_{600} = 0.1$. To determine the MIC of the parent strains (Fig. S7), we added a final

292	concentration of 0, 0.2, 0.5, 1, 2, 4, 8, or 12 μ g/mL to each culture; to determine the MIC of the
293	evolved strains (Fig. S6), we added 0, 0.5, 1, 2, 5, 10, 20, or 50 μ g/mL to each culture. The
294	samples were sealed with evaporation-limiting membranes (Thermo Scientific AB-0580) and
295	grown in 24-well plates at 37°C with 200 rpm orbital shaking. OD ₆₀₀ readings were taken using a
296	BioTek Synergy H1m plate reader before incubation ($t = 0$ h) and after antibiotic exposure ($t = 0$
297	24 h). All experiments were performed in triplicate using biological replicates.

299 Experimental Conditions in the eVOLVER

300 In the eVOLVER, cultures were inoculated from a single colony in LB at 37°C. A stir bar mixed 301 the cultures on a medium setting, or approximately 1000 rpm (34). The LB was supplemented 302 with detergent Tween20 (Sigma Aldrich Cat. # P1379) at 0.2% (v/v) to reduce spurious OD_{600} 303 measurements caused by biofilm growth on the flask.

304

Cells were inoculated in the eVOLVER overnight (t \approx -16 – -14 h) prior to the beginning of the experiment (t = 0 h) to establish steady-state exponential growth. We set the eVOLVER using an upper OD₆₀₀ bound of 0.2 and a lower bound of 0.1; thus, cultures were grown to a turbidity of 0.2 and then diluted back to 0.1 to maintain the turbidostat at approximately constant cell density. Samples were collected during the experiment at set time points (t = 0, 1, 3, 6, 12, 24, 48, and 72 h) and used for downstream analysis. All experiments were performed in triplicate using biological replicates.

312

313 At t = 0 h, we introduced chloramphenicol at a predetermined final treatment concentration 314 ([Cm] = 0, 0.2, 0.5, 1, 2, 5, 10, or 20 μ g/mL). This introduction was implemented by switching 315 the media source from one containing 0 µg/mL chloramphenicol to another containing the final

316 treatment concentration; in addition, we spiked the samples directly with the treatment

317 concentration of chloramphenicol at the same time to avoid a delay due to the time required for

- 318 media cycling in the turbidostat.
- 319

320 Downstream Assays and Data Collection from eVOLVER Samples

321 Growth Rate Measurements

322 Growth rate measurements were calculated after each dilution event using:

Growth Rate =
$$\frac{\ln\left(\frac{OD_{600,high}}{OD_{600,low}}\right)}{t_{OD_{600,high}} - t_{OD_{600,low}}}$$

The growth rate between each dilution was then averaged across sampling time points to compare against disc diffusion assays and spot assays. For example, the growth rate given at t =0 h is the growth rate from t = -6 h to t = 0 h.

326

327 Antibiotic Disc Diffusion Assay

328 We aliquoted samples from the eVOLVER, where the OD_{600} from each sample was between 0.1 and 0.2. We used cotton swabs to cover LB agar plates with a layer of the sample (55). An 329 330 antibiotic disc containing chloramphenicol (30 g) (Thermo Fisher Scientific Cat. # CT0013B) 331 was then placed on the plate. The plate was incubated for 24 h at 37°C. The diameter of the zone 332 of inhibition around each disc was then measured. Diameter of inhibition zones were classified 333 as susceptible, intermediate, or resistant based on Reference (56). Additionally, we calculated the 334 MIC using a linear mapping between MIC and diameter of inhibition zones for our samples 335 (Figure S6) (57).

336

337 Spot Assay

The samples from the eVOLVER experiment were diluted in PBS to the following dilution series: 1, 10^{-1} , 10^{-2} , 10^{-3} , 10^{-4} , and 10^{-5} . We then plated 2.5 µL of each dilution on LB agar plates containing 0, 0.5, 1, 2, 5, 10, and 20 µg/mL chloramphenicol. The plates were then incubated for 24 h at 37°C. To count colonies, we identified the dilution factor with the most countable colonies, and recorded the number of colony forming units (*CFU*) and dilution factor (*d*). The CFU/mL for each sample was then calculated by:

$$CFU/mL = \frac{CFU * d}{V}$$

where *V* is the volume plated. We also calculated the proportion of the population able to grow on different concentrations of chloramphenicol by calculating the CFU/mL from LB agar plates containing 0, 0.5, 1, 2, 5, 10, and 20 μ g/mL chloramphenicol.

347

348 Whole Genome Sequencing

349 DNA was extracted from single isolates and parent strains using the QIAGEN DNeasy 350 PowerBiofilm kit. Samples were sequenced at the Microbial Genome Sequencing Center (MiGS) 351 in Pittsburg, PA, USA, who conducted library preparation based on the Illumina Nextera kit 352 series and then sequenced using a NextSeq 550 platform with 150 bp paired-ends and an average 353 coverage of 50 reads. We analyzed reads using *breseq* (58) version 0.35.1. Sequenced WT 354 isolates were from experiments treated with 2 μ g/mL chloramphenicol in the eVOLVER for 72 h 355 and then isolated on 20 μ g/mL chloramphenicol.

356

357 Data Availability

358	The c	latasets generated during this study are available from the corresponding author upon
359	reason	nable request.
360		
361	ACK	NOWLEDGEMENTS
362	This 1	research was supported by the National Science Foundation (grant No. 1347635) and the
363	Natio	nal Institutes of Health (grant No. R01AI102922).
364		
365	We th	ank Dr. Mo Khalil, Dr. Brandon Wong, Dr. Chris Mancuso, and Zack Heins for their
366	assista	ance and support with the eVOLVER.
367		
368	REFI	ERENCES
369	1.	Smith PA, Koehler MFT, Girgis HS, Yan D, Chen Y, Chen Y, Crawford JJ, Durk MR,
370		Higuchi RI, Kang J, Murray J, Paraselli P, Park S, Phung W, Quinn JG, Roberts TC,
371		Rougé L, Schwarz JB, Skippington E, Wai J, Xu M, Yu Z, Zhang H, Tan MW, Heise CE.
372		2018. Optimized arylomycins are a new class of Gram-negative antibiotics. Nature
373		561:189–194.
374	2.	Sousa MC. 2019. New antibiotics target the outer membrane of bacteria. Nature. NLM
375		(Medline).
376	3.	Imai Y, Meyer KJ, Iinishi A, Favre-Godal Q, Green R, Manuse S, Caboni M, Mori M,
377		Niles S, Ghiglieri M, Honrao C, Ma X, Guo JJ, Makriyannis A, Linares-Otoya L,
378		Böhringer N, Wuisan ZG, Kaur H, Wu R, Mateus A, Typas A, Savitski MM, Espinoza JL,
379		O'Rourke A, Nelson KE, Hiller S, Noinaj N, Schäberle TF, D'Onofrio A, Lewis K. 2019.
380		A new antibiotic selectively kills Gram-negative pathogens. Nature 576:459–464.

381	4.	Hart EM, Mitchell AM, Konovalova A, Grabowicz M, Sheng J, Han X, Rodriguez-Rivera
382		FP, Schwaid AG, Malinverni JC, Balibar CJ, Bodea S, Si Q, Wang H, Homsher MF,
383		Painter RE, Ogawa AK, Sutterlin H, Roemer T, Black TA, Rothman DM, Walker SS,
384		Silhavy TJ. 2019. A small-molecule inhibitor of BamA impervious to efflux and the outer
385		membrane permeability barrier. Proc Natl Acad Sci U S A 116:21748–21757.
386	5.	Luther A, Urfer M, Zahn M, Müller M, Wang SY, Mondal M, Vitale A, Hartmann JB,
387		Sharpe T, Monte F Lo, Kocherla H, Cline E, Pessi G, Rath P, Modaresi SM, Chiquet P,
388		Stiegeler S, Verbree C, Remus T, Schmitt M, Kolopp C, Westwood MA, Desjonquères N,
389		Brabet E, Hell S, LePoupon K, Vermeulen A, Jaisson R, Rithié V, Upert G, Lederer A,
390		Zbinden P, Wach A, Moehle K, Zerbe K, Locher HH, Bernardini F, Dale GE, Eberl L,
391		Wollscheid B, Hiller S, Robinson JA, Obrecht D. 2019. Chimeric peptidomimetic
392		antibiotics against Gram-negative bacteria. Nature 576:452–458.
393	6.	Davies J, Davies D. 2010. Origins and Evolution of Antibiotic Resistance. Microbiol Mol
394		Biol Rev 74:417–433.
395	7.	England PH. 2015. Health Matter – tackling antimicrobial resistance. GOVUK.
396	8.	Ventola CL. 2015. The Antibiotic Resistance Crisis: Part 1: Causes and Threats. Pharm
397		Ther 40:277–283.
398	9.	Toprak E, Veres A, Yildiz S, Pedraza JM, Chait R, Paulsson J, Kishony R. 2013. Building
399		a morbidostat: An automated continuous-culture device for studying bacterial drug
400		resistance under dynamically sustained drug inhibition. Nat Protoc 8:555–567.
401	10.	Toprak E, Veres A, Michel J-B, Chait R, Hartl DL, Kishony R. 2011. Evolutionary paths
402		to antibiotic resistance under dynamically sustained drug selection. Nat Genet 44:101.
403	11.	Alon Cudkowicz N, Schuldiner S. 2019. Deletion of the major Escherichia coli multidrug

404	transporter AcrB reveals transporter plasticity and redundancy in bacterial cells. PLoS
405	One 14:e0218828.

- 406 12. Yoshida M, Reyes SG, Tsuda S, Horinouchi T, Furusawa C, Cronin L. 2017. Time-
- 407 programmable drug dosing allows the manipulation, suppression and reversal of antibiotic
- 408 drug resistance *in vitro*. Nat Commun 8:1–11.
- 409 13. Marchant J. 2018. When antibiotics turn toxic. Nature 555:431–433.
- 410 14. Wistrand-Yuen E, Knopp M, Hjort K, Koskiniemi S, Berg OG, Andersson DI. 2018.
- 411 Evolution of high-level resistance during low-level antibiotic exposure. Nat Commun
- 412 9:1599.
- 413 15. Kohanski MA, DePristo MA, Collins JJ. 2010. Sublethal Antibiotic Treatment Leads to
 414 Multidrug Resistance via Radical-Induced Mutagenesis. Mol Cell 37:311–320.
- 415 16. Andersson DI, Hughes D. 2012. Evolution of antibiotic resistance at non-lethal drug
 416 concentrations. Drug Resist Updat 15:162–172.
- 417 17. Strauss SK, Schirman D, Jona G, Brooks AN, Kunjapur AM, Nguyen Ba AN, Flint A,
- 418 Solt A, Mershin A, Dixit A, Yona AH, Csörgő B, Busby BP, Hennig BP, Pál C,
- 419 Schraivogel D, Schultz D, Wernick DG, Agashe D, Levi D, Zabezhinsky D, Russ D, Sass
- 420 E, Tamar E, Herz E, Levy ED, Church GM, Yelin I, Nachman I, Gerst JE, Georgeson JM,
- 421 Adamala KP, Steinmetz LM, Rübsam M, Ralser M, Klutstein M, Desai MM, Walunjkar
- 422 N, Yin N, Hefetz NA, Jakimo N, Snitser O, Adini O, Kumar P, Smith RSH, Zean R,
- 423 Hazan R, Rak R, Kishony R, Johnson S, Nouriel S, Vonesch SC, Foster S, Dagan T, Wein
- 424 T, Karydis T, Wannier TM, Stiles T, Olin-Sandoval V, Mueller WF, Bar-On YM, Dahan
- 425 O, Pilpel Y. 2019. Evolthon: A community endeavor to evolve lab evolution. PLoS Biol
- 426 17.

427 10. Russ D, Olasel F, Shael Talilal E, Tellil I, Dayili M, Reisic ED, Zalipalolii C	r Tamar E, Yelin I, Baym M, Kelsic ED, Zampaloni C, Haldimann
---	---

- 428 A, Kishony R. 2020. Escape mutations circumvent a tradeoff between resistance to a beta-
- 429 lactam and resistance to a beta-lactamase inhibitor. Nat Commun 11:1–9.
- 430 19. Reding C, Catalán P, Jansen G, Bergmiller T, Rosenstiel P, Schulenburg H, Gudelj I,
- 431 Beardmore R. 2019. Hotspot Dosages of Most Rapid Antibiotic Resistance Evolution.
- 432 bioRxiv 866269.
- 433 20. Delcour AH. 2009. Outer Membrane Permeability and Antibiotic Resistance. Biochim
 434 Biophys Acta 1794:808–816.
- 435 21. Blair JMA, Webber MA, Baylay AJ, Ogbolu DO, Piddock LJ V. 2015. Molecular
- 436 mechanisms of antibiotic resistance. Nat Rev Micro 13:42–51.
- 437 22. Li X-Z, Plésiat P, Nikaido H. 2015. The Challenge of Efflux-Mediated Antibiotic
 438 Resistance in Gram-Negative Bacteria. Clin Microbiol Rev 28:337–418.
- 439 23. Kobylka J, Kuth MS, Müller RT, Geertsma ER, Pos KM. 2020. AcrB: a mean, keen, drug
 440 efflux machine. Ann N Y Acad Sci 1459:38–68.
- 441 24. Nikaido H, Takatsuka Y. 2009. Mechanisms of RND Multidrug Efflux Pumps. Biochim
 442 Biophys Acta 1794:769–781.
- 443 25. Langevin AM, Dunlop MJ. 2018. Stress introduction rate alters the benefit of AcrAB-
- 444 TolC efflux pumps. J Bacteriol 200.
- 445 26. Okusu H, Ma D, Nikaido H. 1996. AcrAB efflux pump plays a major role in the antibiotic
- 446 resistance phenotype of *Escherichia coli* multiple-antibiotic-resistance (Mar) mutants. J
- 447 Bacteriol 178:306–308.
- 448 27. Zwama M, Yamasaki S, Nakashima R, Sakurai K, Nishino K, Yamaguchi A. 2018.
- 449 Multiple entry pathways within the efflux transporter AcrB contribute to multidrug

450 recognition. Nat Commun 9:1–9.

- 451 28. Webber MA, Talukder A, Piddock LJV. 2005. Contribution of mutation at amino acid 45
- 452 of AcrR to *acrB* expression and ciprofloxacin resistance in clinical and veterinary

453 *Escherichia coli* isolates. Antimicrob Agents Chemother 49:4390–4392.

- 454 29. Olliver A, Vallé M, Chaslus-Dancla E, Cloeckaert A. 2004. Role of an *acrR* mutation in
- 455 multidrug resistance of *in vitro*-selected fluoroquinolone-resistant mutants of *Salmonella* 456 *enterica* serovar Typhimurium. FEMS Microbiol Lett 238:267–272.
- 457 30. Wang H, Dzink-Fox JL, Chen M, Levy SB. 2001. Genetic characterization of highly
- 458 fluoroquinolone-resistant clinical *Escherichia coli* strains from China: Role of *acrR*
- 459 mutations. Antimicrob Agents Chemother 45:1515–1521.
- 460 31. Baym M, Lieberman TD, Kelsic ED, Chait R, Gross R, Yelin I, Kishony R. 2016.
- 461 Spatiotemporal microbial evolution on antibiotic landscapes. Science 353:1147–1151.
- 462 32. El Meouche I, Dunlop MJ. 2018. Heterogeneity in efflux pump expression predisposes
 463 antibiotic-resistant cells to mutation. Science 362:686 LP 690.
- 464 33. Lukačišinová M, Fernando B, Bollenbach T. 2020. Highly parallel lab evolution reveals
- that epistasis can curb the evolution of antibiotic resistance. Nat Commun 11:3105.
- 466 34. Wong BG, Mancuso CP, Kiriakov S, Bashor CJ, Khalil AS. 2018. Precise, automated
- 467 control of conditions for high-throughput growth of yeast and bacteria with eVOLVER.
- 468Nat Biotechnol 36:614.
- 469 35. Sood S. 2016. Chloramphenicol A Potent Armament Against Multi-Drug Resistant
- 470 (MDR) Gram Negative Bacilli? J Clin Diagn Res2016/02/01. 10:DC01-DC3.
- 471 36. Nitzan O, Kennes Y, Colodner R, Saliba W, EdelsteinI H, Raz R, Chazan B. 2015.
- 472 Chloramphenicol use and susceptibility patterns in Israel: a national survey. Isr Med

- 473 Assoc J 17:27–31.
- 474 37. Ruiz C, Levy SB. 2013. Regulation of *acrAB* expression by cellular metabolites in
 475 *Escherichia coli*. J Antimicrob Chemother 69:390–399.
- 476 38. Andersson DI, Balaban NQ, Baquero F, Courvalin P, Glaser P, Gophna U, Kishony R,
- 477 Molin S, Tønjum T. 2020. Antibiotic resistance: turning evolutionary principles into
- 478 clinical reality. FEMS Microbiol Rev.
- 479 39. Mcmurry LM, Levy SB. 2013. Amino acid residues involved in inactivation of the
- 480 *Escherichia coli* multidrug resistance repressor MarR by salicylate, 2,4-dinitrophenol, and
- 481 plumbagin. FEMS Microbiol Lett. NIH Public Access.
- 482 40. Grenier F, Matteau D, Baby V, Rodrigue S. 2014. Complete genome sequence of
 483 *Escherichia coli* BW25113. Genome Announc 2.
- 484 41. Hobbs EC, Yin X, Paul BJ, Astarita JL, Storz G. 2012. Conserved small protein associates
- with the multidrug efflux pump AcrB and differentially affects antibiotic resistance. Proc
 Natl Acad Sci U S A 109:16696–16701.
- 487 42. Daley DO, Rapp M, Granseth E, Melén K, Drew D, Von Heijne G. 2005. Global topology
 488 analysis of the *Escherichia coli* inner membrane proteome. Science 308:1321–1323.
- 489 43. Lopes BS, Amyes SGB. 2013. Insertion sequence disruption of *adeR* and ciprofloxacin
- 490 resistance caused by efflux pumps and *gyrA* and *parC* mutations in *Acinetobacter*
- 491 *baumannii*. Int J Antimicrob Agents 41:117–121.
- 492 44. Cannatelli A, D'Andrea MM, Giani T, Di Pilato V, Arena F, Ambretti S, Gaibani P,
- 493 Rossolini GM. 2013. *In vivo* emergence of colistin resistance in *Klebsiella pneumoniae*
- 494 producing KPC-type carbapenemases mediated by insertional inactivation of the
- 495 PhoQ/PhoP *mgrB* regulator. Antimicrob Agents Chemother 57:5521–5526.

496	45.	Durrant M, Li MM, Siranosian B, Bhatt AS. 2019. Mobile genetic element insertions
497		drive antibiotic resistance across pathogens. bioRxiv 527788.
498	46.	Praski Alzrigat L, Huseby DL, Brandis G, Hughes D. 2017. Fitness cost constrains the
499		spectrum of marR mutations in ciprofloxacin-resistant Escherichia coli. J Antimicrob
500		Chemother 72:3016–3024.
501	47.	Ray MJ, Tallman GB, Bearden DT, Elman MR, McGregor JC. 2019. Antibiotic
502		prescribing without documented indication in ambulatory care clinics: national cross
503		sectional study. BMJ 367:16461.
504	48.	Falagas ME, Makris GC, Dimopoulos G, Matthaiou DK. 2008. Heteroresistance: a
505		concern of increasing clinical significance? Clin Microbiol Infect 14:101–104.
506	49.	Hennessy TW, Petersen KM, Bruden D, Parkinson AJ, Hurlburt D, Getty M, Schwartz B,
507		Butler JC. 2002. Changes in Antibiotic-Prescribing Practices and Carriage of Penicillin-
508		Resistant Streptococcus pneumoniae: A Controlled Intervention Trial in Rural Alaska.
509		Clin Infect Dis 34:1543–1550.
510	50.	Čižman M. 2003. The use and resistance to antibiotics in the community. Int J Antimicrob
511		Agents. Elsevier.
512	51.	Kokwaro GO, Muchohi SN, Ogutu BR, Newton CRJC. 2006. Chloramphenicol
513		pharmacokinetics in African children with severe malaria. J Trop Pediatr 52:239–243.
514	52.	Baba T, Ara T, Hasegawa M, Takai Y, Okumura Y, Baba M, Datsenko KA, Tomita M,
515		Wanner BL, Mori H. 2006. Construction of Escherichia coli K-12 in-frame, single-gene
516		knockout mutants: the Keio collection. Mol Syst Biol 2.
517	53.	Datta S, Costantino N, Court DL. 2006. A set of recombineering plasmids for gram-
518		negative bacteria. Gene 379:109–115.

519	54.	Datsenko KA, Wanner BL. 2000. One-step inactivation of chromosomal genes in
520		Escherichia coli K-12 using PCR products. Proc Natl Acad Sci U S A 97:6640–6645.
521	55.	Andrews JM. 2001. BSAC standardized disc susceptibility testing method. J Antimicrob
522		Chemother 48:43–57.
523	56.	Clinical and Laboratory Standards Institute. 2013. M100-S23 Performance Standards for
524		Antimicrobial Susceptibility Testing; Twenty-Third Informational Supplement, 33rd ed.
525		Wayne, PA.
526	57.	Kronvall G. 1982. Analysis of a single reference strain for determination of gentamicin
527		regression line constants and inhibition zone diameter breakpoints in quality control of
528		disk diffusion antibiotic susceptibility testing. J Clin Microbiol 16:784–793.
529	58.	Deatherage DE, Barrick JE. 2014. Identification of mutations in laboratory-evolved
530		microbes from next-generation sequencing data using breseq. Methods Mol Biol
531		1151:165–188.
520		

533 FIGURE CAPTIONS

Figure 1. Evolution experiment schematic. We used the eVOLVER, a modular turbidostat, as an evolutionary platform to measure and record absorbance data at 600 nm (OD₆₀₀). We calculated growth rate after each dilution event and collected samples at defined timepoints (t = 0, 1, 3, 6, 12, 24, 48, 72 h). We performed antibiotic disc assays and spot assays for all samples.

539	Figure 2. Temporal landscapes based on treatment concentration of chloramphenicol. (A)
540	Average growth rate. Growth rates are normalized to growth of strains at $t = 0$ h; for raw data see
541	Figure S1. Lighter areas represent growth rates closer to pre-treatment values; darker areas

represent reduced growth rates. MIC⁰ concentration is denoted with a bold dashed line for each 542 543 strain (Figure S7). (B) Average resistance. Diameter of inhibition zones were plotted for each 544 time and treatment. Smaller inhibition zones are shown in red and correspond to resistant cells 545 (≤ 12 mm) and larger inhibition zones are shown in blue and represent susceptible cells (≥ 19 mm); intermediate inhibition is shown with color scale from orange to green. MIC⁰ is denoted 546 547 with a bold dashed line. (C) Final resistance at 72 h based on treatment concentration normalized to MIC⁰. The calculated MIC^f is based on data from Figure S6. Data points show the mean of 548 549 three biological replicates. Shaded error bars show standard deviation.

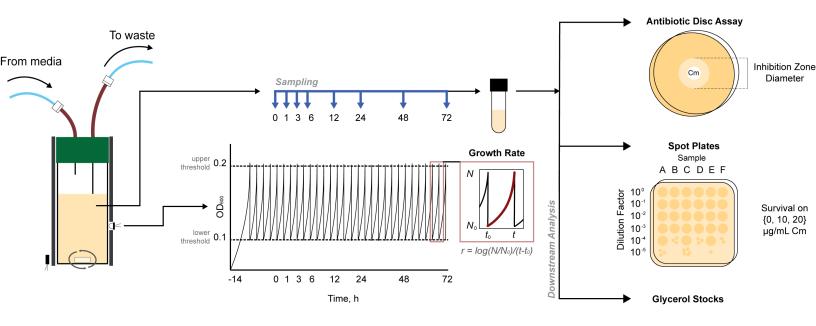
550

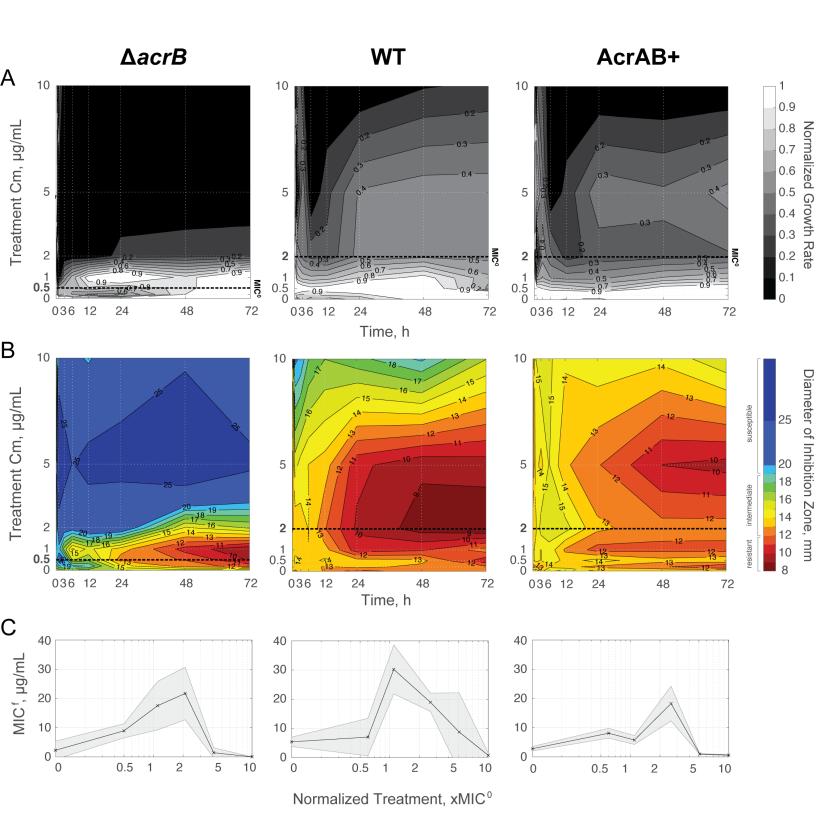
551 Figure 3. Resistance and Fitness Evolution Trajectories. (A) Average diameter of inhibition 552 zone and average growth rate plotted against each other. Lighter purple markers represent 553 trajectories occurring earlier; darker purple are later timepoints. The longer the distance between 554 markers, the greater the change between time points. (B) Schematics summarize patterns for each treatment concentration (xMIC⁰). Schematic plots show growth rate in terms of initial 555 556 growth rate (GR_0) and maximum physiological growth rate (GR_{max}) . Resistance is shown in 557 terms of relative diameter of inhibition, where D_0 is the diameter of inhibition at t = 0 h and D_{min} 558 is the diameter of the antibiotic disc.

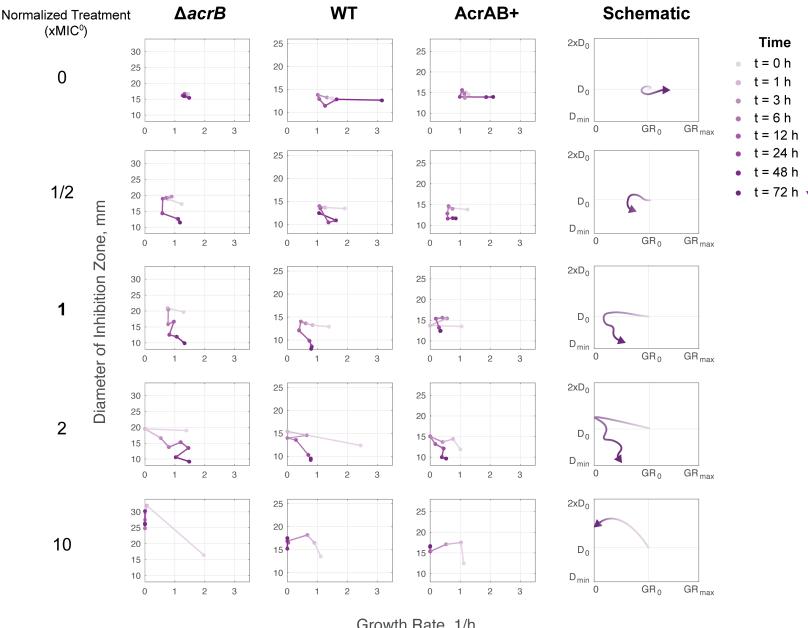
559

Figure 4. Number of Biological Replicates with Highly Resistant Sub-populations through Time. Number of biological replicates that had a subpopulation greater than 5% of their total population, which could grow on LB plates containing (A) 10 μ g/mL or (B) 20 μ g/mL chloramphenicol. Raw data is shown in Figure S3 and data for each replicate at 72 h is shown in Figure S4. Initial populations contained ~10⁷ CFUs. MIC⁰ compared to treatment concentration

565 is denoted with a bold dashed line (Figure S7).







Growth Rate, 1/h

